

NASA Contractor Report 4225

Laser Transit Anemometer Software Development Program

(NASA-CR-4225) LASER TRANSIT ANEMOMETER
SOFTWARE DEVELOPMENT PROGRAM Final Report
(Spectrum Development Labs.) 56 p CSCI 20E

N89-19545

H1/36 Unclas
C197709

John B. Abbiss

CONTRACT NAS1-18311
MARCH 1989

NASA

NASA Contractor Report 4225

Laser Transit Anemometer Software Development Program

John B. Abbiss
Spectron/A Titan Company
Costa Mesa, California

Prepared for
Langley Research Center
under Contract NAS1-18311



National Aeronautics and
Space Administration

Office of Management

Scientific and Technical
Information Division

1989

TABLE OF CONTENTS

| <u>NO.</u> | | <u>PAGE</u> |
|------------|---|-------------|
| | TABLE OF CONTENTS..... | iii |
| | LIST OF FIGURES..... | v |
| | NOMENCLATURE..... | vii |
| 1.0 | INTRODUCTION..... | 1 |
| 1.1 | Program Background: A Historical Review..... | 1 |
| 1.2 | Program Goals..... | 3 |
| 1.3 | Program Summary..... | 3 |
| 2.0 | DEVELOPMENT TASKS..... | 6 |
| 2.1 | Data Acquisition and System Control Software - ACQUIRE..... | 6 |
| 2.2 | Simulation Software - SIMULTAC..... | 6 |
| | 2.2.1 Theoretical Background to SIMULTAC..... | 7 |
| | 2.2.2 Dependence of the Correlation Function on the Flow-Angle Weighting Function and Velocity..... | 11 |
| | 2.2.3 Program Description..... | 12 |
| | 2.2.4 Comment on Threshold Modeling..... | 15 |
| 2.3 | LTA Data Reduction Software - PROCESS..... | 16 |
| | 2.3.1 Renormalization..... | 16 |
| | 2.3.2 Correlogram Filtering..... | 17 |
| | 2.3.3 Correlogram Background Removal..... | 18 |
| | 2.3.4 Transformation of the Data to (V, θ) Space..... | 19 |
| | 2.3.5 Extraction of Flow Parameters..... | 21 |
| | 2.3.6 Multi-station Provisions in the MSCLTA II Software..... | 26 |
| 2.4 | Software Testing..... | 27 |
| 2.5 | Discriminators..... | 32 |
| 3.0 | COMMENTS AND CONCLUSIONS..... | 39 |
| 3.1 | Software Structure..... | 39 |
| 3.2 | Simulations..... | 39 |
| 4.0 | RECOMMENDATIONS..... | 41 |
| 4.1 | Software..... | 41 |
| 4.2 | Hardware..... | 43 |
| 5.0 | REFERENCES..... | 44 |

LIST OF FIGURES

| <u>NO.</u> | | <u>PAGE</u> |
|------------|---|-------------|
| 1 | Transit geometry..... | 8 |
| 2 | Impulse approximated by a 5 V square wave 100 ns wide. This plot shows the response of the detection filter of Board #1..... | 33 |
| 3 | Impulse approximated by a 5 V square wave 100 ns wide. This plot shows the response of the detection filter of Board #2..... | 34 |
| 4 | Impulse approximated by a 5 V square wave 100 ns wide. This plot shows the response of the center estimation filter of Board #1..... | 35 |
| 5 | Impulse approximated by a 5 V square wave 100 ns wide. This plot shows the response of the center estimation filter of Board #2..... | 36 |
| 6 | Impulse approximated by a 5 V square wave 100 ns wide. Total circuit delay from impulse to output is 2400 ns. This plot shows the output delay between Board #1 and Board #2 to be approximately 100 ns..... | 37 |

NOMENCLATURE

| | |
|----------------------|---|
| c | particle concentration in fluid |
| h_n | mean background noise level in simulated correlograms |
| h_p | content of highest channel in simulated correlograms |
| ℓ | axial extent of detector field of view |
| p_{uv} | joint probability density function for u and v |
| $p_{\tau\theta}$ | joint probability density function for τ and θ |
| $p'_{\tau\theta}$ | velocity-biased joint probability density function for τ and θ |
| q | threshold radius: maximum radial distance from beam focus at which a particle is detectable. |
| r_a | distance to beam axis at point of particle's closest approach |
| r_o | beam radius |
| R_j | correlogram at angle setting α_j |
| s | distance between beam foci |
| T_e | duration of an experiment |
| u, v | X- and Y-components of mean velocity of flow in plane normal to beam axis |
| \bar{u}, \bar{v} | mean values of u and v |
| u', v' | r.m.s. fluctuations in u and v |
| V | $\sqrt{u^2 + v^2}$: component of velocity in plane normal to beam axis |
| \bar{V} | mean value of V |
| w | width of the band of particle trajectories which contribute to the correlogram for a given flow angle |
| α | angle between line joining beam foci and X-axis |
| β | angle between particle trajectory and line joining beam foci |
| θ | instantaneous flow direction: angle between particle trajectory and X-axis |
| ρ | correlation coefficient of p_{uv} |
| σ_x, σ_y | standard deviations in u and v |
| τ | correlation function delay time |
| τ_i | delay time at center of i^{th} bin of correlogram (discretized correlation function) |

1.0 INTRODUCTION

1.1 Program Background: A Historical Review

Laser anemometry (or velocimetry-as it is now more commonly identified in the United States) based on the measurement of the time-of-flight of a scattering particle between two laser beams was first discussed in 1968 (Ref. 1). A working implementation of the technique was made by Dr. R. Schodl in West Germany for DFVLR in or about 1971, and his instrument has subsequently been marketed and developed by Polytec GmbH. In their systems, the time-of-flight technique is referred to as the L2F (Laser-two-focus) principle.

In 1973 Dr. A. E. Smart, then of Rolls-Royce Ltd in England, built a two-spot or transit system based on the same principle, but describing the measurement method as laser transit anemometry (LTA), for research measurements in aircraft engine high-speed axial compressors. The L2F/LTA distinction in names is historical. Insofar as there is a difference, it is one of implementation rather than of principle. The major dissimilarity is that in L2F the spot source and conjugate receiver optical stops are rotated separately by a toothed belt drive, whereas the LTA uses an image rotator to spin the image of the test space, leaving both sources and conjugate detector stops fixed. The first image rotator was a doubled-folded Abbé prism but was changed to one using a mirror Dove design for all subsequent machines because of its superior performance with respect to aberrations, transmission efficiency, physical and optical length, and reduced weight. Other major differences were restricted to the way in which the signal was processed.

After joining Spectron Development Laboratories in California in 1977, Dr. Smart redesigned his LTA system and pursued further development of the signal retrieval technique, both theoretically and by building hardware. Beginning in 1978, the Arnold Engineering Development Center supported the initial phase of development of the "Correlex" instrument, designed for ultra-high speed processing of the electrical

signals from laser transmit anemometers and for other physical and chemical applications requiring high-speed correlation techniques. In succeeding years seven LTA systems, based on the Spectron design of the LTA optical head and the Correlex were delivered to NASA, the U.S. Air Force and commercial organizations. All the optical heads were 4" lens diameter units (Model 104) with a range of optical throws from 367 mm to 1600 mm (using interchangeable front lens), except for one 6" unit (Model 106) which had throws of 1 and 4 meters.

The initial 5 ns Correlex correlator concept embodied all the design features of the later units, but not all were then implemented. The first Correlex, appearing as a simple single channel system internally based upon the Intel 80/86 microprocessor, was controlled by a repackaged Apple computer. Capability for multichannel time gating was included from the start, requiring a high-speed external triggering system. Two later systems provided this function internally using a Spectron proprietary phase address card (PAC), which was itself a real time multi-channel sequencing computer. It proved too complex and expensive for all but the most extreme channel switching rates, as, for example, those required in high-speed multi-stage axial compressors. The last machines delivered were controlled by a PDP 11/23 computer, which had basic software for controlling the optical head, data acquisition, display and storage, and some simple nearly-real-time signal retrieval processing.

The Spectron LTA system offered some advantages to complement the already extensive fringe anemometry measurement capabilities at NASA and Air Force Research Centers. LTA offers high accuracy even from small high-velocity particles close to walls, at the expense of measurement time. It has good capability for accurate speed and direction measurement and also for determining the long-term two-dimensional properties of statistically stationary turbulence below about 15%. The application of the LTA instrument to various fluid dynamic situations has shed much light upon the instrument properties and capabilities. These experiments also demonstrated the need for careful interpretation of the

derived measurements and an enhanced understanding of what is now perceived to be a highly complex technology. The detailed study and comparison of data obtained from fringe anemometry and LTA techniques has also given insight into both measurement technologies, as well as the fluid dynamic properties of the flows under examination. This experience has facilitated development of the LTA data processing and information retrieval software now available at NASA and Air Force Research Centers, and has established greater confidence in the results obtainable from LTA systems.

Details of the investigations performed by Spectron for AEDC, which provided much of the background to the developments described in this report, can be found in Ref. 2. Further information relating to the Correlex principles, design and performance is available in Refs. 3 and 4.

1.2 Program Goals

The primary program goal has been to provide working code which will enable the LTA systems to approach the performance in real applications that theoretical analyses suggest should be possible. To meet this objective a number of activities have been undertaken. These included the design of three major software packages; for signal acquisition and system control (ACQUIRE), for data retrieval, processing and archiving (PROCESS), and a data simulation program to permit verification of the processing package (SIMULTAC). Other subsidiary tasks included coding, testing, debugging, verification, and documentation of the above software packages, and the provision of a number of supporting packages and auxiliary routines.

1.3 Program Summary

Earlier SPECTRON work performed for AEDC between April 1st, 1981 and December 31st, 1983 was reported on in Ref. 2. The experimental equipment, consisting of a fully-operational SPECTRON LTA System with the Correlex as supporting signal-processor, was described in four volumes, supplied with the instrument:

- | | | |
|--------|---|------------------|
| Vol. 1 | Optical Head/SDL 81-53003 | - March 1981 |
| Vol. 2 | Correlex Operator's Manual/SDL 82-53010D5 | - October 1982 |
| Vol. 3 | MSCLTA II User's Manual, Version 1.1 | - February 1983 |
| Vol. 4 | MSCLTA II User's Manual, Version 2.0 Rev. | - September 1986 |

The present program was initiated to produce software capable of exploiting the full potential of the SPECTRON LTA System. A major activity was the establishment of a modular architecture within which efficient software development could take place. The importance and validity of this effort are clearly demonstrated by the relatively minor changes that have been found necessary during the course of the program. VAX PASCAL was chosen as the programming language, and the specified target hardware was the VAX 11/730 with VMS operating system. The software structure having been established, a large amount of work was devoted to error trapping, documenting, and rendering robust the code for ACQUIRE and PROCESS. Once this development vehicle was available algorithm development proceeded in the confident expectation that programs would not crash because of unexpected errors in the house-keeping and organizational code. PROCESS, as it was developed to include more of the functional modules, began to reveal problems in running the initial simulation program DAS. As a diagnostic tool, DAS was found to have insufficient power. A new program, SIMULTAC, was conceived and a preliminary version implemented.

The status of the programs delivered at the end of the contract period is as follows:

ACQUIRE is complete, robust and fully operational.

SIMULTAC is as complete as has been found possible with the resources available. There are always, of course, elaborations and enhancements that can be added to simulation, test and diagnostic tools.

PROCESS is complete, robust and fully operational. The embedded algorithms have not been evaluated over a sufficiently wide range to be

sure that they are optimized for their current purpose. More work on the structure of these algorithms and their implementation should result in more powerful and efficient operation, and might make better results available from poorer data. A framework has been constructed within which such improvements may evolve. Specific recommendations can be found in Section 4.

The key objective of the effort was the development in an optimum form of algorithms and related computer codes, together with appropriate documentation, for extracting from the LTA system correlograms obtained in a general three-dimensional flow field the two components u and v of the mean velocity, the root mean square fluctuations u' and v' in these components, and the first-order velocity shear stress $\overline{u'v'}$.

A pair of matched discriminators, designated Channel 8 and having 1.6 microsecond detection filters and 6.4 microsecond center-estimation filters, were to be delivered to Langley for installation and evaluation. A second pair, designated Channel 7 and having 800 nanosecond detection filters and 3.2 microsecond center-estimation filters, were also constructed and delivered to Langley. The characteristics of the discriminator modules available in the Langley instrument are discussed in Section 2.5.

2.0 DEVELOPMENT TASKS

2.1 Data Acquisition and System Control Software - ACQUIRE

In the preliminary versions the entire program for operating the LTA system existed as a single suite of modular code. The decision was taken at an early stage to separate ACQUIRE and PROCESS into two autonomous programs which could be run concurrently within a multi-tasking environment. This option enabled ACQUIRE to be run in real time with no impairment of data acquisition rate, while simultaneously making available selected unprocessed correlograms at the CORRELEX display. System parameters are continuously displayed at the command terminal.

2.2 Simulation Software - SIMULTAC

A major effort was devoted to the further development and refinement of the LTA simulation program SIMULTAC. The program is optimized for speed, using deterministic analytically-based computations to generate the basic correlograms. The effects arising from a finite population of light-scattering particles are simulated by perturbing the correlogram, using a Poisson random number generator. Background noise, assumed to be additive, is generated in the form of appropriately scaled Poisson distributed random numbers.

The basic physical assumptions underlying both the simulation and data-processing software are that:

- (i) the particle's velocity is constant between the light spots;
- (ii) the particle concentration is constant throughout the fluid in space and time;
- (iii) there is negligible relative motion between particle and fluid;
- (iv) the flow is statistically stationary;
- (v) the optical geometry and light intensity distributions are unaffected by the flow properties.

2.2.1 Theoretical Background to SIMULTAC

The geometrical model on which SIMULTAC is based (see Figure 1) assumes two identical light distributions, whose central maxima O_1 and O_2 are separated by a distance s . It is further assumed that the two-dimensional light distribution remains constant in the axial direction, at least over the region of experimental interest. O_1X is the reference axis, in the plane normal to the axis of propagation, from which the orientation α of the line joining the spots is measured.

The circles represent spatial contours within which the scattered light level from a given particle exceeds the threshold of detectability. At present the threshold circle is assumed to have some fixed radius, q ; this is equivalent to making the additional assumptions that all the scattering particles are of the same size and that all particles which pass within a distance q of O_1 or O_2 are detected, whatever the speed. (A modification which would take into account the fact that the light distribution is in reality Gaussian and that faster particles scatter less light is discussed later.) u is the velocity component in the direction O_1X ; v is the orthogonal component in the plane of the diagram. θ and β are the angles made by a general particle trajectory with O_1X and O_1O_2 respectively. Hence:

$$\theta = \alpha + \beta$$

For a particle transit to contribute to the correlogram the corresponding trajectory must intersect both threshold circles. In addition, the transit time (time between points of closest approach to the propagation axes) must be less than the maximum displayed correlogram lag.

We can now calculate the bounds imposed by the threshold constraints on the permissible values of θ .

For a given θ there is a band of width w , say, disposed symmetrically about the line O_1O_2 , which defines those trajectories which make non-zero contributions to the correlogram.

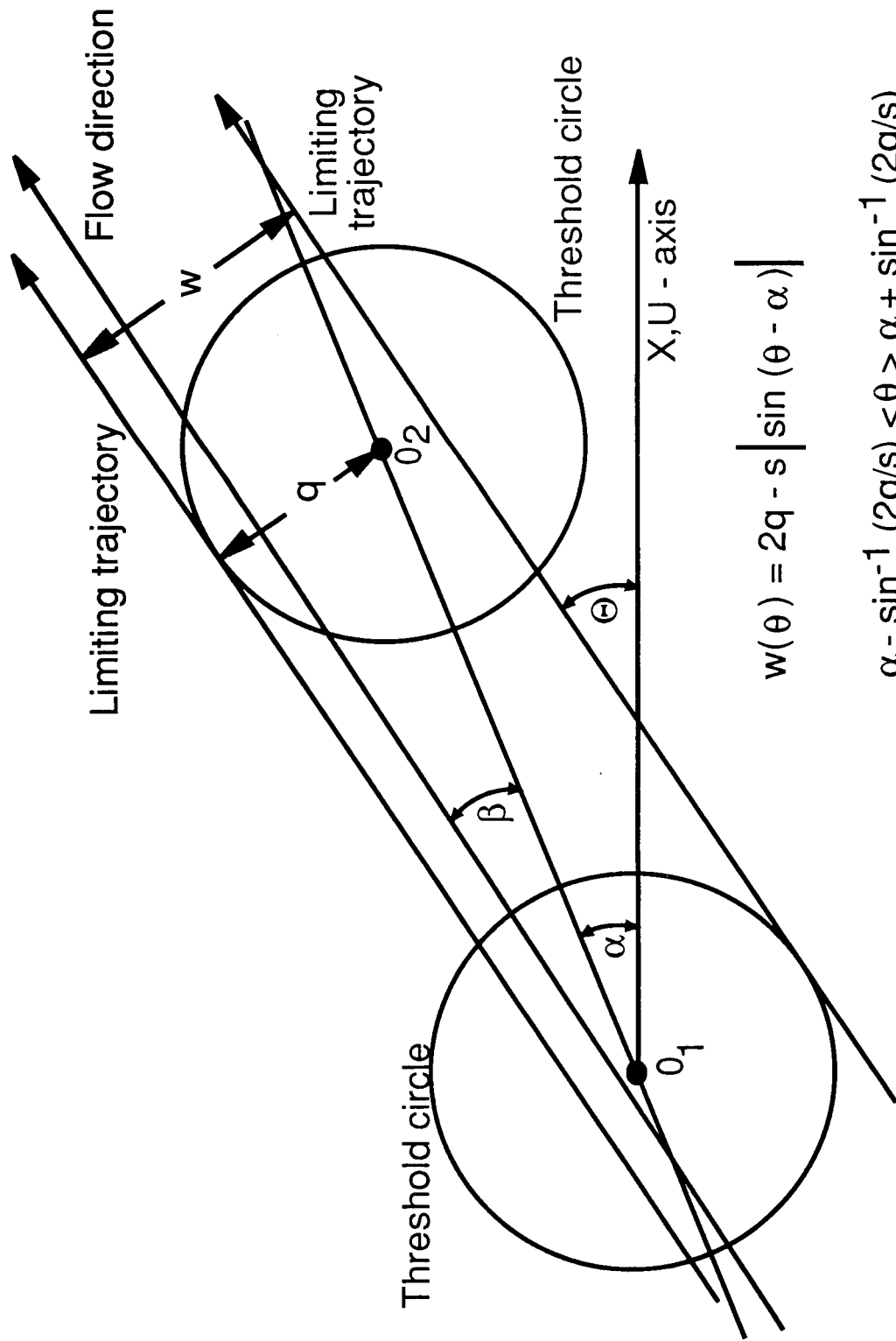


Figure 1. Transit geometry

The extreme trajectories in this band are tangent to one or other of the threshold circles, and from Figure 1,

$$w = 2q - s |\sin \beta|$$

or

$$w = 2q - s |\sin (\theta - \alpha)|. \quad (2.1)$$

Note that $w/2q$ may be interpreted as a probability that an event at the first spot is followed by an event at the second. The maximum permissible absolute value of β is determined by the direction of the particle trajectory for which w becomes zero. Thus,

$$\sin \beta_{\max} = 2q/s,$$

and hence

$$\alpha - \sin^{-1} (2q/s) < \theta < \alpha + \sin^{-1} (2q/s). \quad (2.2)$$

This then determines the range of θ within which a particle trajectory may make a contribution to the correlogram.

The next step is to define the probability density distribution for the velocity components u and v . This function is assumed to be a joint Gaussian random process of the form

$$p_{uv}(u,v) = \frac{1}{2\pi\sigma_x\sigma_y\sqrt{1-\rho^2}} \exp \left[-\frac{1}{2(1-\rho^2)} \left\{ \frac{(u - \bar{u})^2}{\sigma_x^2} - \frac{2\rho(u - \bar{u})(v - \bar{v})}{\sigma_x\sigma_y} + \frac{(v - \bar{v})^2}{\sigma_y^2} \right\} \right], \quad (2.3)$$

where \bar{u} and \bar{v} are the mean values of the velocity components u and v respectively, and σ_x and σ_y are the corresponding standard deviations. ρ is the correlation coefficient, which determines the interdependence of u and v , and is associated with shear stress through the relationship

$$\overline{u'v'} = \rho\sigma_x\sigma_y, \quad (2.4)$$

where u' and v' denote the fluctuating parts of u and v .

In the early versions of SIMULTAC this continuous probability density function was reduced to a two-dimensional histogram of values corresponding to discrete cells (i, j) in (u, v) - space. For the (i,j)th cell

$$\theta = \tan^{-1} (v_j/u_i)$$

and only cells for which this value of θ fell within the range given above contributed to the correlogram.

A major improvement in speed and efficiency was achieved by carrying out the computation of the correlogram directly in (τ, θ) - space. The relationship between the probability distributions in the two spaces is

$$p_{\tau\theta}(\tau, \theta) = \frac{s^2}{\tau^3} p_{uv}(u, v) \quad (2.5)$$

(A table of transformations between various probability distribution spaces is given in Section 2.3.4.)

Then the content of the i th bin of the correlogram at angle setting α_j is computed as

$$R_j(\tau_i) = \int_{\tau_i - 0.5}^{\tau_i + 0.5} \int_{\alpha_j - \Delta\theta}^{\alpha_j + \Delta\theta} \frac{1}{\tau^4} w(\theta) p_{uv}(u = \frac{s}{\tau} \cos \theta, v = \frac{s}{\tau} \sin \theta) d\theta d\tau \quad (2.6)$$

where

$$\Delta\theta = \sin^{-1} (2q/s) ,$$

$$w(\theta) = 2q - s |\sin(\theta - \alpha)| ,$$

and the assumption is made that contributions to the i th bin arise from events whose associated delay times are symmetrically disposed over one sample time around τ_i .

Note that an extra factor τ^{-1} appears in the integrand of Equation (2.6), which represents the effect of velocity - biasing. This formula for $R_j(\tau_i)$, in which the width w of the trajectory acceptance band appears as a weighting function, can be established by the following argument.

2.2.2 Dependence of the Correlation Function on the Flow-Angle Weighting Function and Velocity

We assume that the flow is two-dimensional in the plane normal to the beam axes and that the detector fields of view cover an axial distance l .

Suppose the flow direction is in the range $(\theta, \theta + \delta\theta)$ and the flow velocity is in the range $(V, V + \delta V)$. Then transit times are in the range $(\tau, \tau + \delta\tau)$, where $\tau = s/V$ and s is the spot separation. The probability of occurrence of these conditions is

$$p_{\tau\theta}(\tau, \theta) \delta\tau \delta\theta$$

$$p_{\tau\theta}(\tau, \theta) = \frac{s^2}{\tau^3} p_{uv} \left(u = \frac{s \cos \theta}{\tau}, v = \frac{s \sin \theta}{\tau} \right).$$

effective cross-sectional area presented to the flow is wl where, as

$$w = 2q - s |\sin(\theta - \alpha)|$$

q is the threshold radius.

If the particle concentration is c , the number of particles passing through this area per unit time is, for the given flow conditions,

$$cwlV = cw \frac{s}{\tau}$$

and the contribution to the correlogram in the interval $(\tau, \tau + \delta\tau)$ during an experiment of length T_e is

$$\sum_{\theta} T_e c w \ell \cdot \frac{s}{\tau} \cdot p_{\tau\theta} \delta\tau \delta\theta .$$

Note that the velocity-biasing factor $1/\tau$ has now appeared. In the limit, the contribution to the i th bin of the correlogram at angle setting α_j will be

$$R_j(\tau_i) = T_e c \ell s \int_{\tau_i - 0.5}^{\tau_i + 0.5} \int_{\text{all } \theta} w(\theta) \cdot \frac{1}{\tau} p_{\tau\theta} d\theta d\tau .$$

But $w(\theta)$ is zero outside the range $\alpha_j - \sin^{-1} \frac{2q}{s} < \theta < \alpha_j + \sin^{-1} \frac{2q}{s}$.

Hence

$$R_j(\tau_i) = T_e c \ell s \int_{\tau_i - 0.5}^{\tau_i + 0.5} \int_{\alpha_j - \sin^{-1} \frac{2q}{s}}^{\alpha_j + \sin^{-1} \frac{2q}{s}} w(\theta) \frac{1}{\tau} p_{\tau\theta} d\theta d\tau . \quad (2.7)$$

2.2.3 Program Description

Initial input parameters include the mean flow velocity and direction, the axial and cross-turbulence intensities (standard deviations as percentages of the mean values), and the correlation coefficient, ρ . The number of standard deviations can also be specified at which computation of the correlation function is ended, and all remaining channels are set to zero. The purpose of this feature is to economize on computational time at very low turbulence levels. The LTA system parameters which must be set include spot separation and spot diameter, threshold radius, spot orientation (relative to mean flow), angular increment, number of stores, delay time and acquisition time per correlogram ('stop time').

The simulation then begins by computing a set of correlation functions according to Equation 2.6, which includes the velocity-biasing factor. In the interests of accuracy, the double integral is evaluated for each correlogram bin by Gaussian quadrature, using repeated one-dimensional integration (see, for example, Ref. 5). There are 10 nodes in each integration unless σ_x or σ_y is less than 1%, in which case 20 nodes are used to ensure adequate sampling of the probability distribution function. For some test purposes, a zero threshold may be required. Then $w(\theta)$ is replaced by a delta-function and the double integral becomes an integral over τ alone. The necessary modification to the integration routine is automatically performed in SIMULTAC when a threshold value of zero is chosen.

The operator is then asked whether the correlograms are to be scaled to conform with a specific requirement for the highest channel content, denoted by h_p , of the central correlogram. If not, the program stops, the output at this point consisting of a stored set of noiseless correlograms. The channel contents of each correlogram are non-integral real numbers. If the correlograms are to be scaled, a value for h_p is requested, together with a value for the ratio of mean background noise level h_n to h_p . This background noise is assumed to be flat in the mean, and represents mainly the effects of parasitic radiation in an experiment. (At particle concentrations normally encountered, it can be shown that noise-particle and interparticle correlation events are relatively rare. See also the comments in Section 2.3.3 concerning non-flat backgrounds.)

The next stage of the program consists of scaling the correlograms so that the highest peak takes the value $h_p - h_n$; at this point, the correlograms contain contributions from particle events only. The operator is then asked if 'finite seeding' is to be simulated; i.e., if statistical effects equivalent to those resulting from a limited number of scattering centers are to be included. If not, and if a zero value has been entered for h_n/h_p , execution of the program stops. If finite seeding is required, the correlograms are randomized by means of a

Poisson number generator. The assumption underlying this step is that the particles are purely randomly distributed in the fluid. Then the number of contributions during the experiment from particles within the speed range $(V, V + \delta V)$ will be a Poisson-distributed random variable. For each correlogram bin, the mean of the Poisson process is set equal to the bin content. It should be noted that, since a Poisson process involves integer random numbers, a rounding up or down of the bin contents is necessary.

The total number of particles contributing to the entire correlogram set can now be calculated. Since each correlated particle contributes a '1' to the correlator output, this number is simply the sum of the correlation bin contents over the complete set of correlograms.

If h_n/h_p is zero, execution of the program stops at this point, the output consisting of a set of correlograms in which the only noise source is the finite number of contributing particles. If h_n/h_p is non-zero, a randomized noise background is added to each bin. This is taken to be a Poisson process with mean h_n . The correlograms now represent the result of an experiment involving a finite number of particles and an additive noise background with constant mean. The operator is then asked if jitter noise is to be included in the experiment. This is intended to simulate errors in transit time estimates arising from, for example, low light levels or electron transit time spread or variable gain in the photomultiplier tube, and is only significant at very low turbulence levels. The errors are modeled as a Gaussian random process and are under most experimental circumstances insignificant compared with other noise sources. For this reason, and by mutual agreement, development of this part of the program was given low priority and, although the necessary hooks are in place, coding of the procedure JITTER is largely incomplete. The intended design consisted of a Gaussian randomization of the delay time associated with each count in the correlogram; the resulting random jitter will occasionally move counts into adjacent bins. The standard deviation for the Gaussian process will depend on the discriminators in use (see Section 2.5).

Finally, differing correlogram seeding rates can be simulated. If the 'seeding change' option is selected, each correlogram is scaled by a different random number generated from a Gaussian distribution with a mean of unity and a standard deviation set by the operator. In order to restrict fluctuations to a realistic range, only random numbers within one standard deviation of the mean are accepted by the program. This simulation of fluctuating seeding rates is termed 'denormalization'. As described below, PROCESS includes a compensating 'renormalization' procedure.

2.2.4 Comment on Threshold Modeling

The assumption of a fixed threshold for particle detection in Section 2.1.1 is clearly unsatisfactory. A rather more realistic model can be constructed in the following way.

We retain the assumption that all the particles are of the same size, but now assume that the light distribution in each spot is Gaussian. Since the total quantity of scattered light is inversely proportional to the particle speed V , we shall assume, as a first-order approximation, that the peak of the output from the Gaussian discrimination filter is also inversely proportional to V . A particle transit is detected if this peak exceeds the discriminator threshold setting. To take account of the Gaussian light distribution, a factor $\exp(-2r_a^2/r_o^2)$, where r_o is the beam radius and r_a is the distance to the beam axis at the point of closest approach, must be included in the calculation. Then we can write for the peak height I_p of the filter output

$$I_p = \frac{k}{V} \exp\left(-\frac{2r_a^2}{r_o^2}\right)$$

where k is some constant of proportionality.

Suppose the threshold setting is such that, at the mean speed \bar{V} , a particle is detected when $r_a = q$. Then the criterion for a detection to occur at any other speed is

$$I_p > \frac{k}{v} \exp\left(-\frac{2q^2}{r_o^2}\right),$$

or

$$r_a < q\left(1 - \frac{r_o^2}{2q^2} \log \frac{v}{\bar{v}}\right)^{1/2}.$$

2.3 LTA Data Reduction Software - PROCESS

The following discussion is concerned with the mathematical basis for the sequence of data reduction operations which appear within PROCESS and whose ultimate objective is the extraction of the five flow parameters, consisting of mean velocity components u and v , their r.m.s. fluctuations u' and v' and the first order shear stress $u'v'$. The main stages in the reduction of the data are:

1. Renormalization of correlogram set
2. Correlogram filtering
3. Correlogram background removal
4. Transformation of the data to (V, θ) space
5. Extraction of flow parameters

2.3.1 Renormalization

Variations in the rate of acquisition of data from one angle setting to another can result in a partially random scaling within a given set of experimental correlograms. Simulation of this feature of the physical LTA environment, referred to in the program comments as denormalization, is available as an option in SIMULTAC.

To compensate for these data rate fluctuations, processing of the data currently begins with a renormalization stage. The peak correlogram value y_i for each angle setting θ_i is located and a best fit found to the Gaussian formula

$$y_1 = c \exp \left\{ - \frac{(\theta_1 - \theta_0)^2}{2\eta^2} \right\}$$

where c , θ_0 and η are unknown constants. Each correlogram is then rescaled by the new peak value. Note that the assumption that the points lie on a Gaussian curve may not be strictly correct. Numerical experiments with simulated data, however, suggest that the approximation is a very good one.

2.3.2 Correlogram Filtering

A self-adaptive digital filter is used to smooth the raw data. A triangular (Parzen) weighting function is used, which has better peak-preserving properties than a rectangular shape and, hence, provides better performance at low turbulence levels. The background level for each correlogram is first estimated by averaging over the data between the third store and the store nearest to 0.6 times the peak store number. After subtracting this average level the remaining data are summed, giving an estimate of the total signal content, Q say, of the correlogram. If H is the peak store content, the half-width of the filter is defined as

$$HW = \text{ROUND} \left(\beta \frac{Q}{2H} \right),$$

where the operation ROUND makes HW an integer. β is an empirical constant which provides control over the broadening induced by the filter. Any filtering, of course, involves a compromise between noise reduction and loss of signal detail. Further investigation of the relationship between turbulence level and the optimum value for β is clearly desirable.

Having determined HW , the filter is now applied to the original correlogram data. Each data point $Y(k)$ is replaced by a triangularly weighted average over the set of data points from locations $k - HW$ to $k + HW$ according to the formula

$$Y(k) \leftarrow \frac{1}{HW} \sum_{j = k - HW}^{j = k + HW} \left(1 - \frac{|k - j|}{HW}\right) Y(j).$$

The filtering computation is carried out in the procedure FILTER in the ALGORITHM module.

2.3.3 Correlogram Background Removal

During the course of this work much discussion has been devoted to the problems of dealing with background noise in the correlation data. Unfortunately, some characteristics found in experimental data are not fully understood; for example, background levels may differ significantly at small and large delay times, and sloping backgrounds have been observed on a number of occasions. The basic assumptions are made in PROCESS that the background can, for most purposes, be reasonably well approximated by a horizontal correlogram floor, and that the signal content does not occupy more than the central 50% of the correlogram. Accordingly, the means of the contents of two groups of channels, occupying the initial and final 20% of the correlation function, are calculated and compared. The greater is taken as the effective overall noise level. The channel numbers at which the central correlogram peak decays to the noise level are also determined at this stage. After subtraction of the background, the correlogram is truncated by setting all channel contents to zero beyond these points. The computations are performed in the ALGORITHM module in procedure BACKGROUND.

If, in a particular experiment, the correlogram background is not flat, the effect of these numerical procedures will be to overcompensate for the noise and reduce the signal contribution. For unimodal velocity distributions, mean values will probably not be greatly affected, but higher moments will certainly become unreliable.

2.3.4 Transformation of the Data to (V, θ) Space

To clarify the discussion, Table 2.1 is included here to show the relationships between the various spaces in which the velocity probability density function can be expressed. These relationships are governed by the modulus of the Jacobian of the appropriate transformation, $|J|$.

TABLE 2.1

| FUNCTION SPACE | | $ J $ | PDF RELATIONSHIPS |
|----------------|--------|--------------|---|
| INPUT | OUTPUT | | |
| (u, v) | (V, θ) | V | $P_{V\theta} = V P_{uv}$ |
| (u, v) | (τ, θ) | s^2/τ^3 | $P_{\tau\theta} = \frac{s^2}{\tau^3} P_{uv}$ |
| (τ, θ) | (V, θ) | τ^2/s | $P_{V\theta} = \frac{\tau^2}{s} P_{\tau\theta}$ |
| (τ, θ) | (u, v) | τ^3/s^2 | $P_{uv} = \frac{\tau^3}{s^2} P_{\tau\theta}$ |

The variables in the table have their conventional meanings and are related by the formulas

$$\begin{aligned}
 u &= V \cos \theta, & v &= V \sin \theta, \\
 V &= \sqrt{u^2 + v^2}, & \theta &= \arctan (v/u), \\
 \tau &= s/V.
 \end{aligned}$$

It is appropriate at this point to correct an error appearing in Ref. 2; on Page 33, the factor τ^4 should be replaced by τ^3 in Equations (4.7) and (4.8).

All the flow information is, of course, available in any of the spaces of Table 2.1. The choice of space in which to carry out the data-processing will be governed in practice by a number of considerations, including noise characteristics, the significance of nonuniform spacing of samples, interpolation or truncation problems and computational burden. It is not possible, on the basis of present experience, to make very general recommendations, but a scheme which operates almost entirely in (u,v) space and which is based on weaker assumptions than the present procedures is described in Section 4.1.

Velocity-biasing should be considered in the treatment of experimental data. As demonstrated above (see Section 2.2.2) for the simple fixed-threshold detection model, the unbiased distribution function can be recovered by including an additional division by velocity, or, equivalently, multiplication by τ/s . (See also Ref. 6) For example, the transformation from (τ, θ) space to (V, θ) space is given by

$$p_{V\theta}(V, \theta) = \frac{\tau^2}{s} p_{\tau\theta}(\tau, \theta) . \quad (2.8)$$

If $p'_{\tau\theta}$ represents the biased distribution function obtained from experiment, we then have

$$p_{V\theta}(V, \theta) = \frac{\tau^3}{s^2} p'_{\tau\theta}(\tau, \theta) . \quad (2.9)$$

In a Correx-LTA system, each detected transit is represented by a single pulse at the appropriate delay time. Hence, in the absence of noise and given adequate sampling of the flow, the final correlogram should have the same form as the biased distribution function expressed in (τ, θ) coordinates; i.e., it should be proportional to $p'_{\tau\theta}$. Thus, a section through the $p_{V\theta}$ distribution can be recovered directly from the correlogram by the use of Equation (2.9).

In the current version of PROCESS, the correlograms are transformed from (τ, θ) space to (V, θ) space before the required flow parameters are extracted. The necessary transformation of the τ -coordinates into V -coordinates is accomplished using the formula

$$i_V = \text{TRUNC} \left[\frac{16641}{i_\tau + 1} - 1 \right]$$

where i_τ is the correlogram channel number and i_V the corresponding channel number in V -space. Note that $16641 = (256 \times 65) + 1$. The '1' is added to ensure that a significant error is not introduced when the divisor is a factor of 16640. Only channel numbers 64-225 are converted in this way (into channel numbers 255-64 in V -space), the assumption being that there are no signal contributions to the correlogram for $i_\tau = 0-63$. The data in V -space, now non-uniformly spaced, are also taken to be zero for $i_V = 0-63$.

2.3.5 Extraction of Flow Parameters

The correlation function in (τ, θ) space has now been transformed into an unnormalized section through the velocity probability density function in (V, θ) space. The succeeding stage of data-processing consists of extracting from each of the transformed correlograms, at angle settings θ_j , the peak height H_j , peak position P_j , the sum of the channel contents Q_j and the first and second moments of velocity V_j and T_j , respectively. The best parabolic fit is then found to the 5 highest values of the set $\{H_j\}$, using the equation

$$H = a_1 \theta^2 + b_1 \theta + c_1 \quad (2.10)$$

At the highest point (H_0, θ_0) of this curve $dH/d\theta = 0$, giving as the most probable flow angle

$$\theta_o = -b_1/2a_1 .$$

$$\text{Then } H_o = c_1 - \frac{b_1^2}{4a_1} .$$

This calculation is based on the assumption that the velocity distribution can be well approximated near the peak by a parabola. This is not unreasonable for a joint Gaussian function. We shall also assume that θ_o is a good approximation to the mean flow angle.

Having found θ_o , the nearest five angle settings can be identified. A second parabolic fit is now performed on the five values of V_j associated with these angles, using

$$V = a_2 \theta^2 + b_2 \theta + c_2 . \tag{2.11}$$

Having thus determined a_2 , b_2 and c_2 , the mean speed is taken to be

$$V_o = a_2 \theta_o^2 + b_2 \theta_o + c_2 .$$

We now have our estimates of mean flow speed and direction. Estimates of σ_x , σ_y , and ρ are obtained by locating pairs of points in each transformed correlogram (still in (V,θ) space) which lie on the contour of the velocity distribution function at some given level. In the current version of PROCESS this level is $1/\sqrt{e}$ times the highest point H_o of the distribution.

This choice was originally made because the slope of the probability density function is a maximum at this plane, and the sensitivity of the data points to noise is minimized. Selecting a lower level, however, has the advantage of generating more intersections, and the choice is not necessarily optimal.

The basic assumption here is that each correlogram in (V, θ) space can be described by a Gaussian. Although not strictly true if ρ is significantly non-zero, the errors are probably very small for contours at the $1/\sqrt{e}$ level. Hence, we write for the j th transformed correlogram

$$Y = H_j \exp \left\{ - \frac{(V - V_j)^2}{2T_j^2} \right\} \quad (2.12)$$

The $1/\sqrt{e}$ plane is at an absolute height of H_o/\sqrt{e} . Setting Y equal to this value, we obtain for the pair of points on the contour

$$V_{ej} = V_j \pm T_j \left[-2 \log (H_o/H_j \sqrt{e}) \right]^{1/2}$$

Pairs of points can be obtained in this way from all correlograms for which $H_j > H_o/\sqrt{e}$. The coordinates (V_{ej}, θ_j) are finally transformed, also in procedure KARY, to (u, v) space by means of the relations

$$\begin{aligned} u_{ej} &= V_{ej} \cos (\theta_j - \theta_o) , \\ v_{ej} &= V_{ej} \sin (\theta_j - \theta_o) . \end{aligned} \quad (2.13)$$

Referring the angular settings to θ_o aligns the v -axis with the mean flow. The derived values for σ_x and σ_y will now represent the required axial- and cross-turbulence magnitudes respectively.

It should be noted here that there is an error in the procedure described above. The pairs of points at the $1/\sqrt{e}$ level should be found in (u, v) space, not (V, θ) space, since the transformation from one space to the other alters the shape of the probability distribution function. The appropriate Jacobian is given by Table 2.1.

The parameters σ_x , σ_y and ρ are obtained by the following argument.

Equation (2.3) represents the model for the normalized velocity probability density function. An arbitrary scaling factor is introduced in the case of the function, p'_{uv} say, describing the experimental data:

$$p'_{uv} = h_0 \exp \left[- \frac{1}{2(1-\rho^2)} \left\{ \frac{(u - \bar{u})^2}{\sigma_x^2} - 2\rho \frac{(u - \bar{u})(v - \bar{v})}{\sigma_x \sigma_y} + \frac{(v - \bar{v})^2}{\sigma_y^2} \right\} \right] \quad (2.14)$$

At the $1/\sqrt{e}$ contour level

$$p'_{uv} = h_0 / \sqrt{e} .$$

Hence the equation for this contour, an ellipse, is

$$\frac{(u - \bar{u})^2}{\sigma_x^2} - 2\rho \frac{(u - \bar{u})(v - \bar{v})}{\sigma_x \sigma_y} + \frac{(v - \bar{v})^2}{\sigma_y^2} = 1 - \rho^2 . \quad (2.15)$$

Differentiating, we find

$$\frac{dv}{du} = \frac{\sigma_y^2 (u - \bar{u}) - \rho \sigma_x \sigma_y (v - \bar{v})}{\rho \sigma_x \sigma_y (u - \bar{u}) - \sigma_x^2 (v - \bar{v})} .$$

$$\frac{dv}{du} = \infty \text{ when}$$

$$\rho \sigma_x \sigma_y (u - \bar{u}) = \sigma_x^2 (v - \bar{v})$$

Substituting in Equation (2.15) we obtain

$$u = \bar{u} + \sigma_x \quad (2.16)$$

When $\frac{dv}{du} = 0$ we obtain

$$v = \bar{v} + \sigma_y \quad (2.17)$$

Hence σ_x and σ_y can be found from the points on the ellipse at which the tangents are parallel to the coordinate axes.

When $v = \bar{v}$, Equation (2.15) gives

$$\rho = \left[1 - \frac{(u - \bar{u})^2}{\sigma_x^2} \right]^{1/2} \quad (2.18)$$

Hence ρ can be found from either of the points of intersection of the ellipse with the u -axis. As described above (see Equation (2.13)), the coordinate axes are chosen so that $\bar{v} = 0$.

The final steps in the present procedure for computing σ_x , σ_y and ρ then consist of a least squares fit of an ellipse to the set of points given by Equation (2.13), finding the points at which the tangents to this ellipse are parallel to the axes, finding a point on the u -axis at which $v = 0$, and finally applying Equations (2.16), (2.17) and (2.18).

If a contour is chosen at some height other than the $e^{-1/2}$ level, say at e^{-b} , it can easily be shown that Equations (2.16) to (2.18) become

$$(u - \bar{u})^2 = 2b\sigma_x^2 \quad \text{when } \frac{dv}{du} = \infty$$

$$(v - \bar{v})^2 = 2b\sigma_y^2 \quad \text{when } \frac{dv}{du} = 0$$

$$\rho = \left[1 - \frac{(u - \bar{u})^2}{2b\sigma_x^2} \right]^{1/2} \quad \text{when } v = \bar{v}.$$

Finally, the comment may be added that σ_x , σ_y and ρ can be derived directly from the coefficients found in carrying out the elliptical fit to the data. The equation on which this procedure is based is

$$c_1 u^2 + c_2 v^2 + c_3 uv + c_4 u + c_5 v = 1 .$$

By expanding Equation (2.15) and comparing coefficients, we find

$$\sigma_x = 2 \frac{c_2(1 + c_1 \bar{u}^2)^{1/2}}{4c_1 c_2 - c_3^2}$$

$$\sigma_y = 2 \frac{c_1(1 + c_1 \bar{u}^2)^{1/2}}{4c_1 c_2 - c_3^2}$$

$$\rho = -c_3/2 (c_1 c_2)^{1/2}$$

Similar formulas can be found for contours at other than the $1/\sqrt{e}$ level.

2.3.6 Multi-station Provisions in the MSCLTA II Software

The original design of the MSCLTA II software included provisions for the control of a Correlex system containing a PAC card for multi-station data acquisition. To verify that the multi-station provisions did indeed work, a simulated test flow was set up at SPECTRON, where multi-station acquisition was successfully performed. Communication was established and data sets transferred from the Correlex to the VAX and stored.

Following the first software delivery to the NASA Lewis facility, the Correlex equipment was set up. NASA Lewis provided a test flow to demonstrate the functionality of both single and multi-station acquisition modes. Once again, data were successfully acquired. However, some communication problems were encountered with the Lewis arrangement that were not detected with the SPECTRON configuration, primarily in the setting of certain PAC card front panel parameters.

While the PROCESS portion of the MSCLTA II software was being developed, the simulation program was modified to produce correlogram

data sets imitating a multi-station acquisition mode. This permitted testing of multi-station features in the PROCESS program. It is believed that the multi-station mode functions as intended, and demonstrated at the Lewis facility, although the analysis of data using PROCESS in the multi-station mode has not been performed as extensively as for the single-station mode.

2.4 Software Testing

A restricted set of software tests has been conducted. A strategy was developed with the goal of achieving a working SIMULTAC/PROCESS combination which met certain performance criteria. SIMULTAC and PROCESS were demonstrated initially on ideal data and subsequently with a limited number of contributing particles and with background noise. Performance criteria included the following:

- (i) Both computers involved - SPECTRON's VAX 11/730 and IBM PC/AT - should yield the same results with common software.
- (ii) Output estimates for \bar{V} , θ , σ_x , σ_y and ρ should improve in accuracy with increasing numbers of particles, reducing turbulence and reducing noise levels.
- (iii) Repeated trials with noise data should reveal no biases.

The test parameters used for (i) and (ii) are set out in Table 2.2. Some statistical tests were also carried out for the two turbulence levels and for $h_p = 500$, $h_n/h_p = 0.1$. The results of all these trials are included as Tables 2.3, 2.4 and 2.5. It can be seen that, for the IBM and VAX 11/730 computers, the performance criteria have been generally well met.

Table 2.2. SIMULTAC/PROCESS Test Cases

| | |
|--|------------------------|
| Spot Separation | 852 micron |
| Spot Diameter | 40 micron |
| Threshold Radius | 0, 1, 15 micron |
| Delay time | 200 ns |
| Number of Stores | 256 |
| Mean Velocity | 30 ms ⁻¹ |
| Mean Flow Orientation | 0 degrees |
| Axial Turbulence | 1,5 % |
| Cross Turbulence | |
| Correlation Coefficient | 0.4 |
| Angular Steps | 9 |
| Angular Increment | 0.15° at 1% turbulence |
| 1.1° at 5% turbulence | |
| Height of Correlogram Peak, h_p | 500, 100 |
| Fractional Background Level, h_n^p/h_p | 0, 0.1, 0.5 |

TABLE 2.3
 IBM/VAX COMPARATIVE RESULTS USING SIMULTAC AND PROCESS PROGRAMS

VELOCITY = 30.00 ms⁻¹; $\sigma_x = \sigma_y = 1.00\%$; $\rho = 0.40$

| RUN NO. | THRESHOLD SETTING (μm) | h_p | h_n/h_p | OUTPUT ESTIMATES (IBM/VAX) | | | | | |
|---------|-------------------------------------|--------------|-----------|------------------------------------|----------------------------------|----------------|----------------|-----------|--|
| | | | | MEAN VELOCITY (ms^{-1}) | MEAN FLOW DIRECTION ($^\circ$) | σ_x (%) | σ_y (%) | ρ | |
| 25 | 0 | (∞) | 0 | 29.995/29.995 | -0.04/-0.04 | 1.07/1.07 | 1.07/1.07 | 0.40/0.40 | |
| 23 | | 500 | 0.1 | 30.007/30.001 | -0.03/-0.01 | 1.11/1.32 | 0.94/1.92 | 0.35/0.67 | |
| 24 | | 500 | 0.5 | 29.998/29.980 | -0.05/-0.03 | 1.20/0.99 | 0.98/0.84 | 0.36/0.21 | |
| 21 | | 100 | 0.1 | 29.997/30.001 | -0.01/ 0.06 | 1.05/1.23 | 1.09/1.06 | 0.41/0.42 | |
| 22 | | 100 | 0.5 | 31.770/29.817 | -0.00/-0.72 | 1.34/0.59 | 1.47/0.00 | 0.56/0.00 | |
| 30 | 2 | (∞) | 0 | 29.995/29.995 | -0.04/-0.04 | 1.07/1.07 | 1.07/1.07 | 0.40/0.40 | |
| 28 | | 500/400 | 0.1 | 29.986/29.975 | -0.07/ 0.00 | 1.08/1.31 | 0.95/1.04 | 0.31/0.44 | |
| 29 | | 500 | 0.5 | 30.008/29.979 | 0.04/-0.05 | 1.20/1.14 | 1.03/1.04 | 0.49/0.44 | |
| 26 | | 100 | 0.1 | 30.023/30.000 | -0.05/-0.04 | 1.10/1.18 | 0.95/1.19 | 0.28/0.37 | |
| 27 | | 100 | 0.5 | 35.153/30.057 | 0.00/-0.05 | 1.02/1.58 | 0.56/1.11 | 0.31/0.10 | |
| 35 | 30 | (∞) | 0 | 29.999/29.999 | -0.06/-0.06 | 1.05/1.05 | 1.89/1.86 | 0.20/0.20 | |
| 33 | | 500 | 0.1 | 29.998/30.005 | -0.02/-0.10 | 1.10/1.12 | 2.19/2.17 | 0.30/0.20 | |
| 34 | | 500 | 0.5 | 29.996/29.986 | 0.23/-0.25 | 1.21/1.11 | 1.87/1.38 | 0.09/0.26 | |
| 31 | | 100 | 0.1 | 29.980/34.550 | -0.04/ 0.37 | 1.10/0.87 | 2.12/5.64 | 0.27/0.42 | |
| 32 | | 100 | 0.5 | 34.276/30.053 | 0.45/ 0.05 | 0.91/1.22 | 0.00/1.09 | 0.00/0.27 | |

TABLE 2.4
 IBM/VAX COMPARATIVE RESULTS USING SIMULTAC AND PROCESS PROGRAMS

VELOCITY = 30.00 MS⁻¹; $\sigma_x = \sigma_y = 5.00\%$; $\rho = 0.40$

| RUN N.O. | THRESHOLD SETTING (μm) | h_p | h_n/h_p | OUTPUT ESTIMATES (IBM/VAX) | | | | |
|-------------|---|--------------|-----------|--|--|-------------------|-------------------|-----------|
| | | | | MEAN VELOCITY (ms^{-1}) | MEAN FLOW DIRECTION ($^\circ$) | σ_x (%) | σ_y (%) | ρ |
| 12 | 0 | (∞) | 0 | 30.067/30.067 | 0.03/ 0.03 | 5.03/5.03 | 5.04/5.04 | 0.40/0.40 |
| 14 | | 500 | 0.1 | 30.112/30.060 | 0.07/-0.01 | 4.93/4.98 | 4.90/5.18 | 0.41/0.42 |
| 13 | | 500 | 0.5 | 30.117/30.152 | 0.22/ 0.16 | 5.16/5.00 | 5.65/5.22 | 0.45/0.31 |
| 16 | | 100 | 0.1 | 30.180/30.046 | 0.21/ 0.06 | 4.94/5.25 | 5.13/4.73 | 0.36/0.40 |
| 15 | | 100 | 0.5 | 25.436/30.070 | -0.87/ 0.58 | 5.11/0.00 | 0.00/2.25 | 0.00/0.00 |
| VAX only | | 100 | 0.5 | -/30.287 | -/ 0.04 | -/4.93 | -/4.92 | -/0.57 |
| 215 | | 100 | 0.5 | -/30.017 | -/ 0.09 | -/4.34 | -/5.14 | -/0.44 |
| 11 | 2 | (∞) | 0 | 30.067/30.067 | 0.03/ 0.03 | 5.03/5.05 | 5.04/5.04 | 0.40/0.40 |
| 8 | | 500 | 0.1 | 30.091/30.063 | -0.09/ 0.06 | 4.93/5.22 | 5.64/4.92 | 0.44/0.34 |
| 7 | | 500 | 0.5 | 30.111/30.055 | 0.15/-0.07 | 4.75/4.87 | 5.06/5.26 | 0.38/0.44 |
| 10/110 | | 100 | 0.1 | 30.112/30.043 | 0.13/-0.04 | 4.92/5.03 | 4.96/4.58 | 0.42/0.36 |
| 9 | | 100 | 0.5 | 34.979/29.913 | 0.73/-0.46 | 3.23/5.37 | 3.04/5.68 | 0.04/0.57 |
| 6 | 30 | (∞) | 0 | 30.066/30.066 | 0.02/ 0.02 | 5.03/5.05 | 5.26/5.26 | 0.38/0.38 |
| 3 | | 500 | 0.1 | 30.113/30.055 | 0.02/ 0.07 | 4.93/5.12 | 4.96/5.14 | 0.38/0.38 |
| 1 | | 500 | 0.5 | 30.069/30.089 | 0.01/ 0.11 | 4.86/4.89 | 4.77/4.81 | 0.37/0.36 |
| IBM only | | 500 | 0.5 | 30.103/- | 0.10/- | 4.82/- | 5.89/- | 0.39/- |
| 5 | | 100 | 0.1 | 30.117/30.054 | 0.16/ 0.31 | 4.89/4.95 | 5.15/6.40 | 0.46/0.48 |
| 4 | | 100 | 0.5 | 30.502/30.140 | 0.02/ 0.39 | 5.55/13.08 | 4.64/6.45 | 0.29/0.45 |
| VAX only | | 100 | 0.5 | -/30.040 | -/ -0.46 | -/4.50 | -/6.60 | -/0.42 |

TABLE 2.5
STATISTICAL TESTS (VAX COMPUTER)

Input Parameters:

Mean Velocity = 30 ms⁻¹
 Threshold Diameter = 30 μm
 Greatest Channel Content (h_n) = 500
 Fractional Background Level^P(h_n/h_p) = 0.1

Output Estimates for $\sigma_x = \sigma_y = 5\%$

| Run No. | Velocity Estimate (ms ⁻¹) | Flow Direction | σ_x | σ_y | ρ |
|-----------|---------------------------------------|----------------|------------|------------|--------|
| STAT005/1 | 30.076 | 0.06 | 4.98 | 5.33 | 0.37 |
| 2 | 30.017 | -0.02 | 5.18 | 5.07 | 0.35 |
| 3 | 30.067 | 0.01 | 5.07 | 5.52 | 0.39 |
| 4 | 30.064 | 0.04 | 5.01 | 5.23 | 0.37 |
| 5 | 30.056 | -0.02 | 4.92 | 5.13 | 0.38 |
| 6 | 30.055 | -0.03 | 4.95 | 5.45 | 0.38 |
| 7 | 30.076 | 0.01 | 5.01 | 5.27 | 0.38 |
| 8 | 30.093 | 0.04 | 4.99 | 4.91 | 0.37 |
| 9 | 30.072 | 0.11 | 5.05 | 5.44 | 0.39 |
| 10 | 30.052 | -0.04 | 4.99 | 5.48 | 0.41 |

Output Estimates for $\sigma_x = \sigma_y = 1\%$

| Run No. | Velocity Estimate (ms ⁻¹) | Flow Direction | σ_x | σ_y | ρ |
|-----------|---------------------------------------|----------------|------------|------------|--------|
| STAT001/1 | 30.001 | -0.12 | 1.13 | 1.74 | 0.25 |
| 2 | 29.999 | -0.12 | 1.07 | 1.98 | 0.17 |
| 3 | 29.993 | -0.11 | 1.15 | 2.00 | 0.33 |
| 4 | 29.999 | 0.06 | 1.07 | 1.65 | 0.17 |
| 5 | 30.003 | -0.05 | 1.19 | 3.05 | 0.46 |
| 6 | 30.005 | -0.03 | 1.13 | 1.79 | 0.21 |
| 7 | 29.991 | -0.04 | 1.13 | 1.86 | 0.27 |
| 8 | 30.006 | -0.03 | 1.13 | 1.68 | 0.20 |
| 9 | 30.011 | 0.05 | 1.20 | 1.39 | 0.14 |
| 10 | 29.995 | -0.06 | 1.11 | 1.95 | 0.22 |

2.5 Discriminators

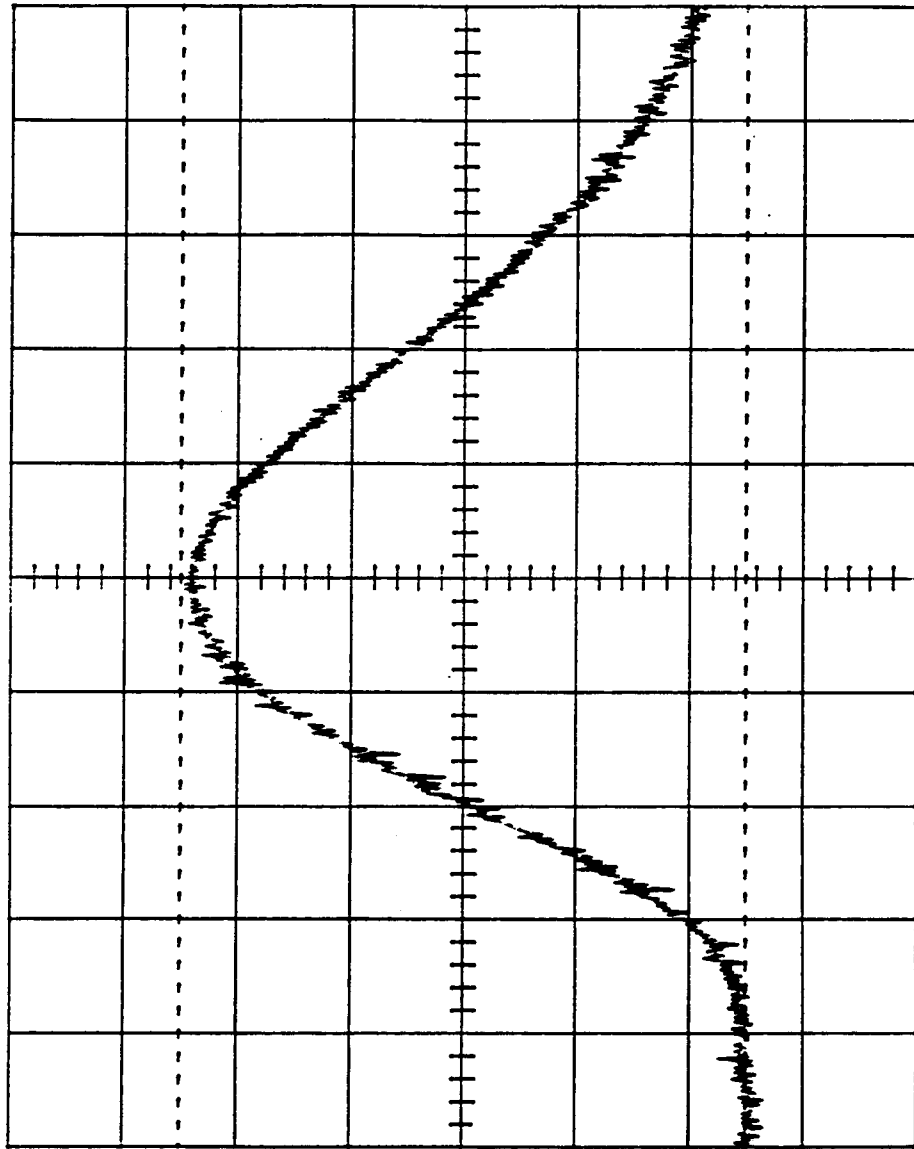
As part of the third-year contract, additional discriminator hardware was provided to extend the LTA equipment capabilities to include lower speed flows. Each of the six discriminator modules on a discriminator card, of which there are two in the optical head, is intended for a specific speed range, with a factor of two between ranges. Each discriminator is designed to be compatible with flow speeds from one-half to twice the center value, although the performance is acceptable over a range several times greater than this. The six pairs of discriminator filter modules originally supplied to NASA Langley are described in Section VI of SDL 81-53003 (Optical Head), March 1981, which was provided with the original LTA equipment. The ranges originally covered were identified as 1 through 6; the ranges of the two new filter modules supplied under the present contract are designated 7 and 8. The characteristics of the detection filters and center estimation filters are shown in Table 2.6.

Table 2.6.

| <u>Slot</u> | <u>Range No.</u> | <u>Detection Filter Width</u> | <u>Center Estimation Filter Width</u> |
|-------------|------------------|-------------------------------|---------------------------------------|
| A | 1 | 15 ns | 50 ns |
| B | 2 | 25 ns | 100 ns |
| C | 3 | 50 ns | 200 ns |
| D | 4 | 100 ns | 400 ns |
| E | 5 | 200 ns | 800 ns |
| F | 6 | 400 ns | 1.6 μ s |
| - | 7 | 800 ns | 3.2 μ s |
| - | 8 | 1.6 μ s | 6.4 μ s |

Figures 2-6 which relate to the Range 7 discriminators, are included to illustrate typical performance features.

Main
Menu

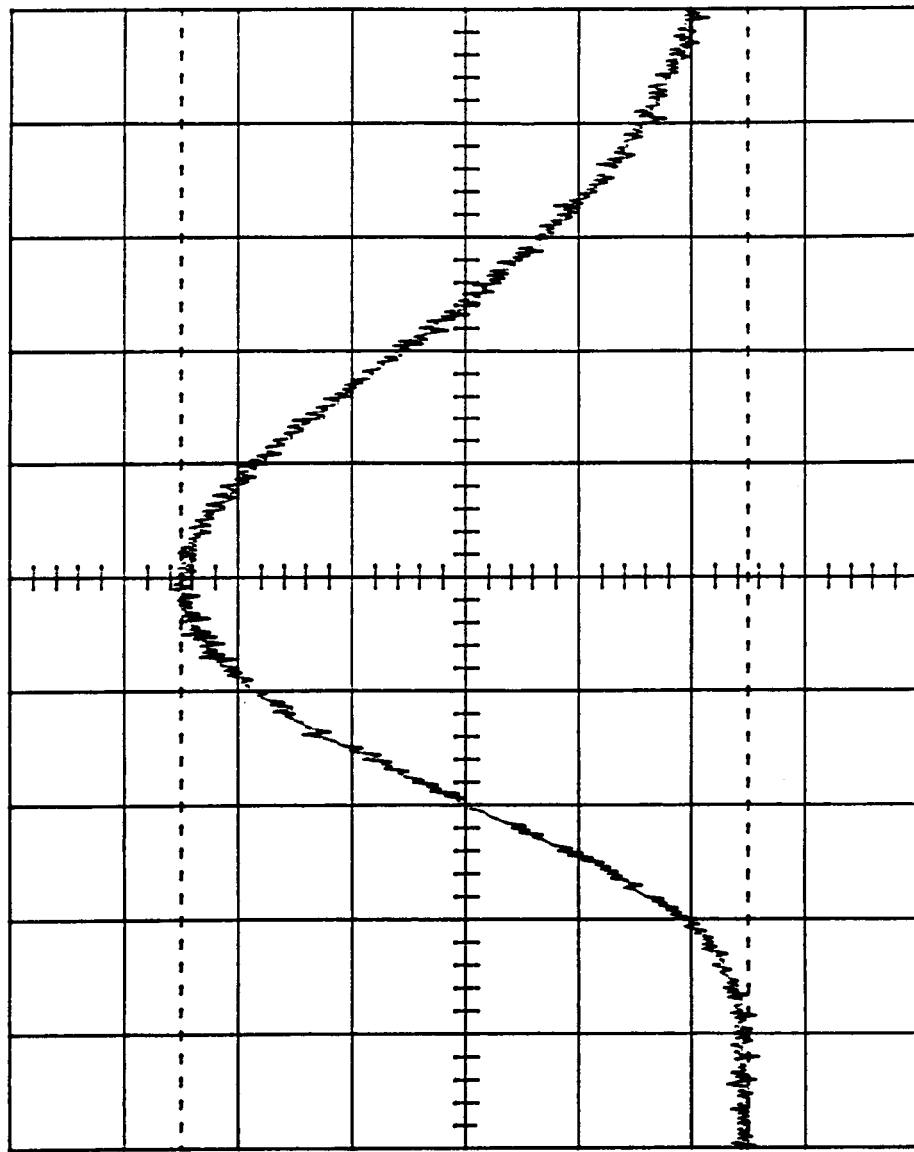


Channel 1
.1 μ s 20 mV

Ch 1 20 mV =
T/div .1 μ s Ch 2 .5 V =
Trig 1.80 div + CHAN 1 ~

Figure 2. Impulse approximated by a 5 V square wave 100 ns wide. This plot shows the response of the detection filter of Board #1.

Main
Menu

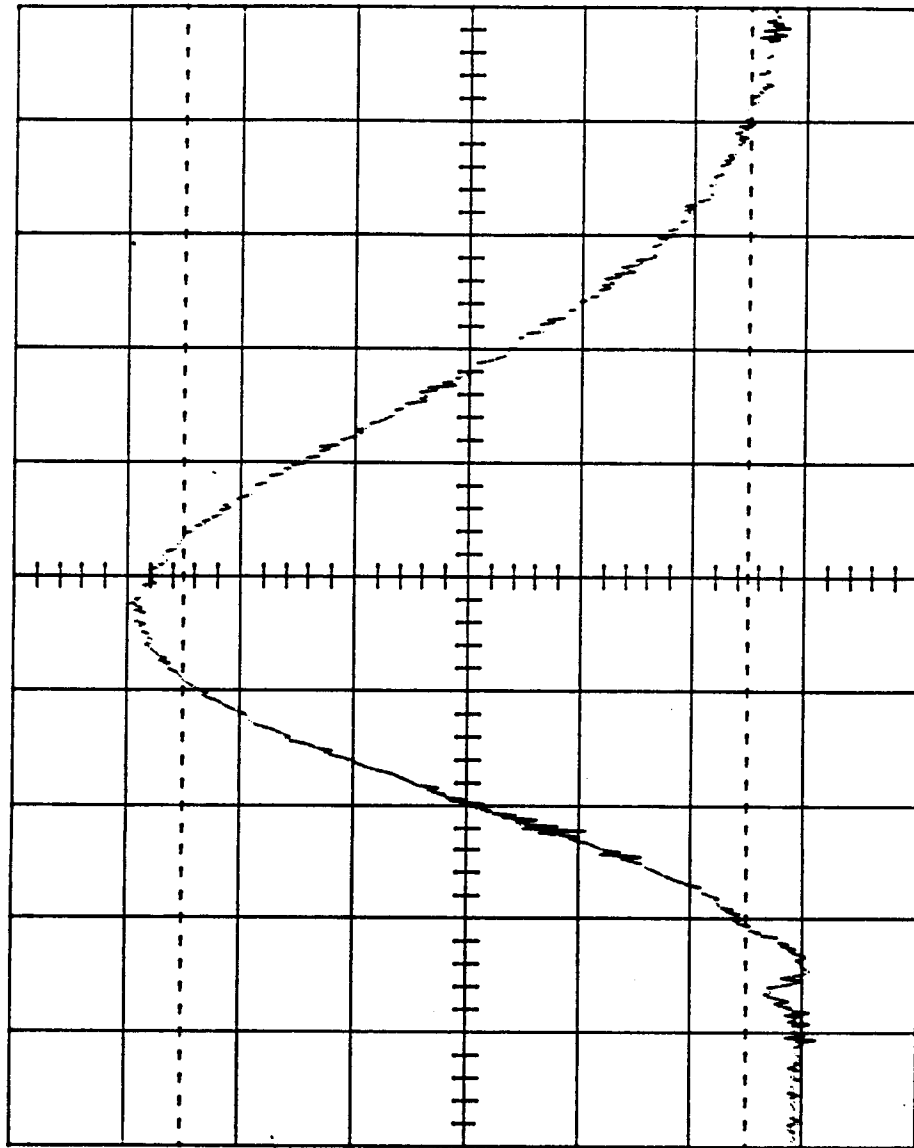


Channel 1
.1 μ s 20 mV

Ch 1 20 mV =
T/div .1 μ s Ch 2 .5 V =
Trig 1.32 div + CHAN 1 ~

Figure 3. Impulse approximated by a 5 V square wave 100 ns wide. This plot shows the response of the detection filter of Board #2.

Main
Menu



Channel 1
.5 μ s 5 mV

Ch 1 5 mV =
T/div .5 μ s Ch 2 5 mV =
Trig- .04 div + CHAN 1 ~

Figure 4. Impulse approximated by a 5 V square wave 100 ns wide. This plot shows the response of the center estimation filter of Board #1.

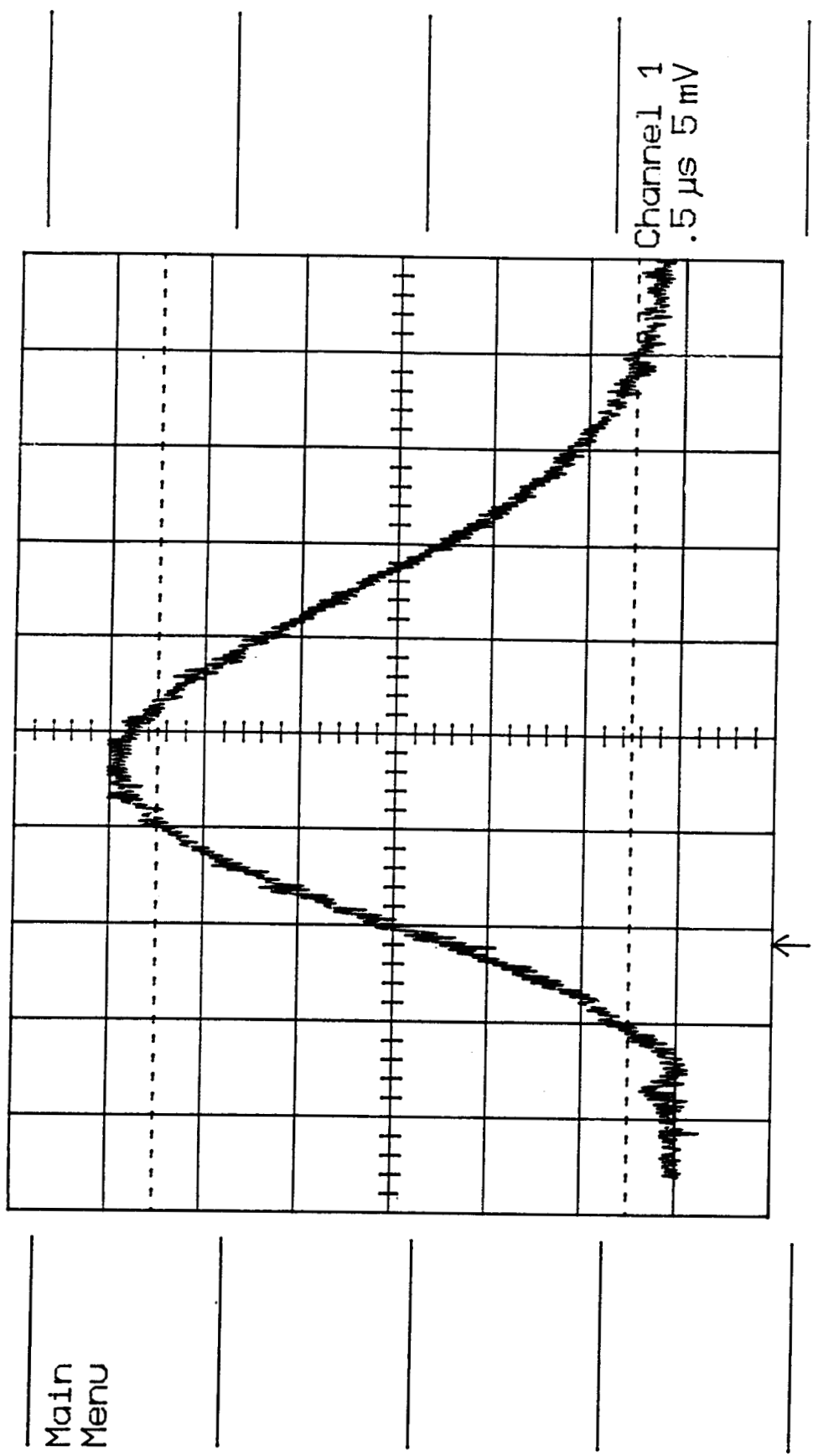


Figure 5. Impulse approximated by a 5 V square wave 100 ns wide. This plot shows the response of the center estimation filter of Board #2.

Main
Menu

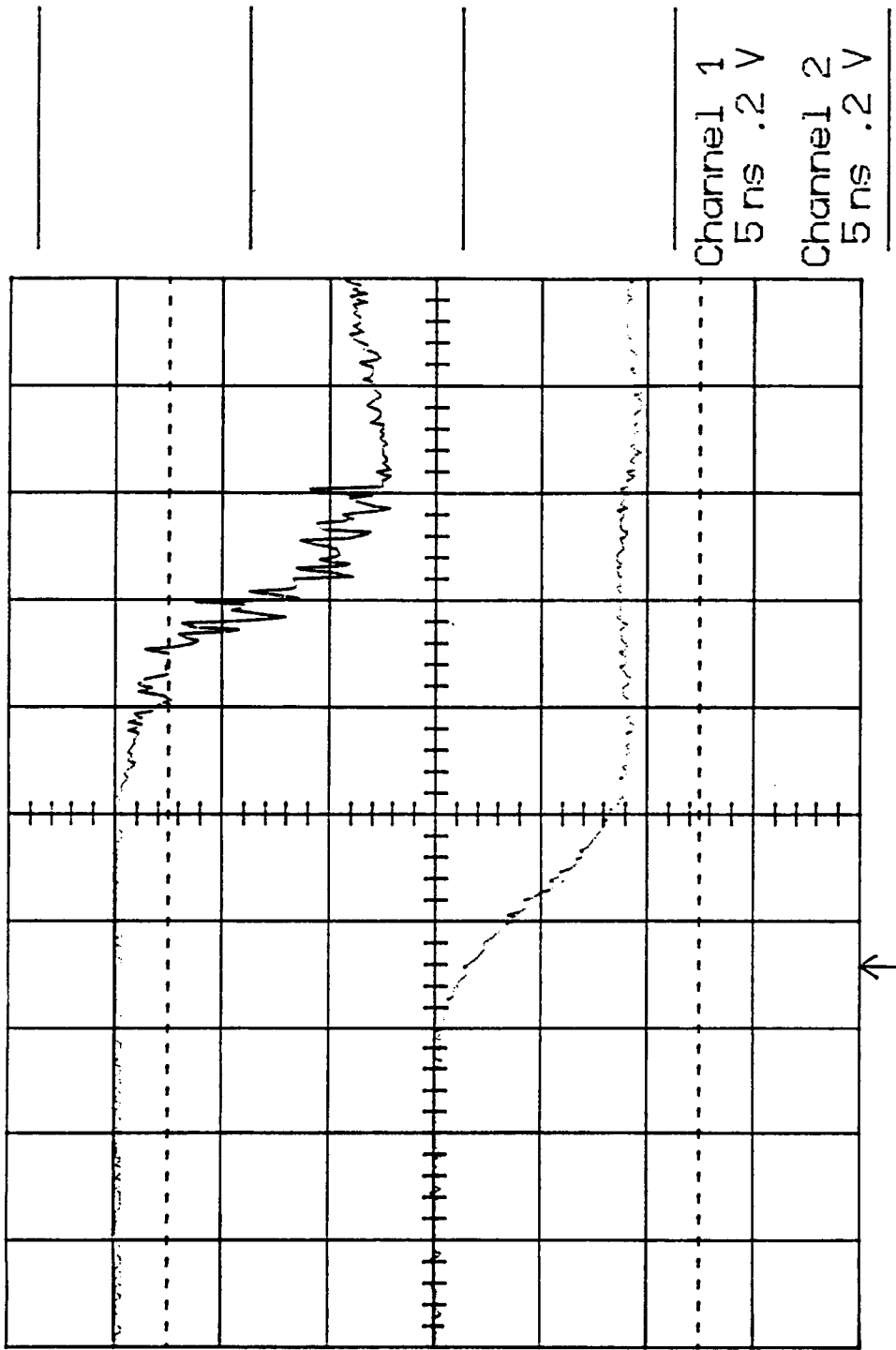


Figure 6. Impulse approximated by a 5 V square wave 100 ns wide. Total circuit delay from impulse to output is 2400 ns. This plot shows the output delay between Board #1 and Board #2 to be approximately 10 ns.

A brief description of the operation of the discriminators was given in the Manual referred to above. A more detailed discussion can be found in Ref. 7.

3.0 COMMENTS AND CONCLUSIONS

3.1 Software Structure

At the beginning of this program it was realized that success or failure in creating a usable set of software depended on a clear understanding of its intended function. Indeed, the process of 'design' has been described as 'understanding the requirements.' The value of the detailed discussions of the framework of the software structure, which occupied so much of the initial effort, has been demonstrated by the fact that the architecture has subsequently remained essentially unchanged. Several modules have undergone some alterations, and cosmetic work is still needed, but the skeleton is fixed and has proved appropriate for the task.

The separation of the data acquisition program, ACQUIRE, from the information retrieval program, PROCESS, was an early and significant development. Its value is obvious in retrospect. The first reportable activity consisted of generating a user-acceptable interface; as a result, many of the software operations, while accessible to the dedicated analyst, are transparent to the user in routine applications. This early planning made the final programs easy to maintain, and the generation of the necessary documentation a straightforward task.

It should be noted that, in its present form, ACQUIRE assumes that the resources of a VAX multi-tasking environment are available. For the convenience of users of more basic systems, ACQUIRE would need to be modified to include some simple processing capabilities.

3.2 Simulations

The effort that has gone into simulation has demonstrated the importance of planning, in the early stages of the program, the structure and functions of the testing and validation methods to be used in the evaluation of the data-processing software. Since this program was

initiated a great deal of knowledge and experience has been gained in these areas, and the need to devote adequate resources to the creation of a computer model reflecting as faithfully as possible the physical properties of the primary data is now clearly appreciated. Attempting to model the LTA system in all its material aspects would, however, have been an unacceptably labor-intensive task in the present program and some simplifications and approximations have been inevitable. For example, including all the properties of a full three-dimensional flow field would raise far too many complications, and the underlying assumption was therefore made that the flow is purely two-dimensional in the plane normal to the transmitter axis. Eventual extension to include three-dimensional effects on particle transits would, of course, be highly desirable.

4.0 RECOMMENDATIONS

4.1 Software

While the delivered software is complete and operational, our primary recommendation is to give priority to the program of testing, confirmation and verification in order to gain confidence that the programs really do what they are supposed to do, particularly with imperfect data. It remains necessary to inspect the correlograms visually to decide whether processing should continue or whether the data should be discarded. The criteria on which this choice is made, and which should be incorporated in the code have not been quantitatively identified, and the degree of dependence on the experience of the operator remains higher than is really desirable. Progress towards reliable fully-automated software will depend on a thorough understanding of the procedures in PROCESS and any shortcomings that may remain. Close technical liaison among users is also very important.

In particular we recommend that PROCESS is exercised on high quality data over as large a range of values of the various parameters as possible, and only subsequently on progressively poorer data. The full test matrix is given in Table 4.1.

The least satisfactory aspect of PROCESS in its present form is the underlying assumption that the flow can be modeled as a correlated bivariate Gaussian random process. This will certainly not be true in some cases - for example, in shear flows or where shock waves are present. A radical solution to this problem of general applicability would be to replace all the procedures following the initial conditioning of the correlograms (filtering, background removal and truncation) with a model-free spline fit.

Table 4.1. Complete Test Matrix

| | |
|--|---------------------------|
| Spot Separation | 852 micron |
| Spot Diameter | 40 micron |
| Delay Time | 5 ns - 1 μ s |
| Number of Stores | 256 |
| Mean Velocity Components: | |
| u | 2 - 1000 ms^{-1} |
| v | 2 - 1000 ms^{-1} |
| Turbulence Components: | |
| σ_x | 0 - 30% |
| σ_y | 0 - 30% |
| Correlation Coefficient | -1 to +1 |
| Angular Steps | 3 |
| Angular Increment | 0.02° - 5° |
| Height of Correlogram Peak, h_p | 10 - 104 |
| Fractional Background Level, h_n/h_p | 0.05 - 0.5 |

A modification to the existing data-reduction procedure for Gaussian flows, which has rather more generality and which operates in (u,v) space, is recommended as a simpler solution and has the following structure:

- (i) precondition correlograms in (τ, θ) space with present algorithms but in the order: filter, remove background, renormalize.
- (ii) transform to (u,v) space.
- (iii) find peak height H_j at each angle θ_j and its coordinates (u_j, v_j) .
- (iv) fit Nth order polynomial ($N = 4$ may be a good choice) to the H_j as a function of θ_j and find peak H_0 and corresponding angle θ_0 ; this is taken to be the mean flow direction.
- (v) fit Nth order polynomial to the set $\{(u_j, v_j)\}$.
- (vi) find intersection of ray at θ_0 with this curve; this gives mean flow speed.
- (vii) find $1/\sqrt{\epsilon}$ points (or points at some other level) from correlograms in (u,v) space.
- (viii) perform elliptical fit as at present to find σ_x , σ_y and ρ .

Implementing such a scheme would not involve major alterations to the structure of the present software.

4.2 Hardware

Enhancements to the hardware which would improve the available accuracy in the estimation of turbulence could be made with existing technology.

The first possibility is to modify the present Correlex by introducing a known delay into the "A" channel. This has the effect of shifting the correlogram data to the left since the transit times are apparently smaller. The delay time per store may then be reduced to spread the data over a larger number of stores. Limitations on this technique are that the delay time cannot be less than 5 nanoseconds and that the "A" channel delay must be known to an accuracy consistent with that required for the measurements.

Secondly, new correlators have been designed and constructed using a timing principle which is not based on discretization of time into set intervals. These instruments are capable of much improved accuracy and use a digital implementation of the former analog LTA filter/discriminators, together with improved algorithms. The processing of the event interval data is based on the Correlex principle.

5.0 REFERENCES

1. Thompson, D. H., "A Tracer Particle Fluid Velocity Meter Incorporating a Laser." J. Sci. Inst. (J. Phys. E), Series 2, Vol. 1, 929-932, (1968).
2. Smart, A. E. and Mayo, W. T., "Techniques for the Measurement of Turbulence and High-Speed Flow with a Laser Transit Anemometer:" Volume I (Technical). Arnold Engineering Development Center Technical Report AEDC-TR-84-13, Volume I, May 1984.
3. Mayo, W. T., Jr., Woodward, R. P., Boland, A., and Smart, A. E., "CORRELEX, A Multiplexed Correlation Processor." Paper 17, Proceedings, 4th International Conference on Photon Correlation Techniques in Fluid Mechanics, Stanford University, Stanford, California, 25-27 August 1980.
4. Mayo, W. T., Jr., and Smart, A. E., "Limitations of LTA Technology at Mach 8; Theory and Practice." Paper XXVI, Proceedings, Symposium on Long Range and Short Range Optical Velocity Measurements, German-French Research Institute, Saint-Louis, France, 15-18 September 1980.
5. Press, William H., et al, "Numerical Recipes: The Art of Scientific Computing." Cambridge University Press, Cambridge and New York, 1986.
6. McLaughlin, D. K., and Tiederman, W. G., "Biasing Correction for Individual Realization of Laser Anemometer Measurements in Turbulent Flow." Phys. Fluids, Vol. 16, 2082 (1973).
7. Smart, A. E., and Mayo, W. T., Jr., "Photon Processing Requirements and Technology for Laser Transmit Anemometry." Paper 10, as Ref. 3.



Report Documentation Page

| | | | |
|---|--|--|---------------------------------|
| 1. Report No. NASA CR-4225 | 2. Government Accession No. | 3. Recipient's Catalog No. | |
| 4. Title and Subtitle Laser Transit Anemometer Software Development Program | | 5. Report Date March 1989 | 6. Performing Organization Code |
| | | 8. Performing Organization Report No. SDL 88-2513-27F/76 | |
| 7. Author(s) John B. Abbiss | | 10. Work Unit No. 505-61-01 | |
| | | 11. Contract or Grant No. NAS1-18311 | |
| 9. Performing Organization Name and Address Spectron/A Titan Company 3535 Hyland Avenue Costa Mesa, CA 92626-1489 | | 13. Type of Report and Period Covered Contractor Report | |
| | | 14. Sponsoring Agency Code | |
| 12. Sponsoring Agency Name and Address National Aeronautics and Space Administration Langley Research Center Hampton, Virginia 23665-5225 | | 15. Supplementary Notes Langley Technical Monitor: William W. Hunter, Jr. Final Report | |
| 16. Abstract Algorithms have been developed for the extraction of two components of mean velocity, standard deviation, and the associated correlation coefficient from laser transit anemometry (LTA) data ensembles. The solution method is based on an assumed two-dimensional Gaussian probability density function (PDF) model of the flow field under investigation. The procedure consists of transforming the data ensembles from the data acquisition domain (consisting of time and angle information) to the velocity space domain (consisting of velocity component information). The mean velocity results are obtained from the data ensemble centroid. Through a least squares fitting of the transformed data to an ellipse representing the intersection of a plane with the PDF, the standard deviations and correlation coefficient are obtained. A data set simulation method is presented to test the data reduction process. Results of using the simulation system with a limited test matrix of input values is also given. | | | |
| 17. Key Words (Suggested by Author(s)) Laser Velocimetry | | 18. Distribution Statement Unclassified-Unlimited Subject Category 36 | |
| 19. Security Classif. (of this report) Unclassified | 20. Security Classif. (of this page) Unclassified | 21. No. of pages 56 | 22. Price A04 |